Journal of Solid State Chemistry **154,** 329–337 (2000)
doi:10.1006/jssc.2000.8789, available online at http://www.idealibrary.com on IDEAL®

The Order of the Palladium and Germanium Atoms in the Germanides *Ln*PdGe (*Ln* = La–Nd, Sm, Gd, Tb) and the New Compound $Yb_3Pd_4Ge_4$

Dirk Niepmann, Yurii M. Prots', Rainer Pöttgen,[1] and Wolfgang Jeitschko[1]

Anorganisch-Chemisches Institut, Universität Münster, Wilhelm-Klemm-Straße 8, D-48149 Münster, Germany

Received March 9, 2000; in revised form May 16, 2000; accepted May 26, 2000; published online August 11, 2000

In previous publications about the seven ternary equiatomic title compounds only the KHg_2 ($CeCu_2$)-type subcells with statistical distribution of the palladium and germanium atoms were reported. However, weak superstructure reflections resulting from an ordered distribution of these atoms are observed in the Guinier powder patterns. A CaCuGe (α-YbAuGe)-type structure with a tripled subcell *b* axis was established from the powder patterns for the compounds LaPdGe, CePdGe, PrPdGe, NdPdGe, SmPdGe, and the low-temperature (α) modification of GdPdGe. In addition, this structure was refined from single-crystal X-ray diffractometer data of CePdGe: *Pnma*, $a = 2190.2(9)$ pm, $b = 448.4(2)$ pm, $c = 767.3(3)$ pm, $R = 0.019$ for 396 structure factors and 56 variable parameters. The refinement of this structure for α-GdPdGe resulted in $a = 2112.3(3)$ pm, $b = 440.5(1)$ pm, $c = 757.7(1)$ pm, $R = 0.022$ for 372 *F* values and 56 variables. The high-temperature (β) modification of GdPdGe has a YPdSi-type superstructure with a doubled *b* axis of the subcell: *Pmmn*, $a = 430.3(1)$ pm, $b = 1409.9(2)$ pm, $c = 757.6(1)$ pm, $R = 0.019$ for 470 *F* values and 40 variables. In spite of the long-range order of the palladium and germanium atoms established for the superstructures, the refinements of the occupancy parameters suggest small amounts of Pd/Ge disorder for all compounds. The crystal chemistry of these compounds is briefly discussed. The new germanide $Yb_3Pd_4Ge_4$ was prepared from the elements in a sealed tantalum tube in a high-frequency furnace and its structure was refined from single-crystal X-ray data: $Gd_3Cu_4Ge_4$ type, *Immm*, $a = 410.7(1)$ pm, $b = 707.0(1)$ pm, $c = 1372.2(3)$ pm, $R = 0.027$ for 667 *F* values and 23 variables.

Key Words: **palladium germanides; crystal structure; superstructures.**

INTRODUCTION

Equiatomic rare earth palladium germanides have intensively been investigated in recent years with respect to phase analytical relationships and physical properties (1–18). The most interesting compound in this series is the dense Kondo system CePdGe which orders antiferromagnetically at 3.4 K (3–7). On the basis of X-ray and neutron powder diffraction data, a disordered KHg_2 ($CeCu_2$)-type structure (19, 20) has been assumed for the whole series of compounds *Ln*PdGe. An exception in this series is EuPdGe (10) which crystallizes with the monoclinic EuNiGe-type structure. This germanide contains divalent europium (21).

In some recent papers we reported on several superstructures with pronounced KHg_2-type subcells (22–27). In the course of our studies of equiatomic rare earth palladium silicides *Ln*PdSi (24, 26) and rare earth platinum germanides *Ln*PtGe (27) we decided to search also for the suspected superstructures in the series of the germanides *Ln*PdGe reported to be isotypic with KHg_2. Precise X-ray powder data of the compounds *Ln*PdGe (*Ln* = La–Nd, Sm, Gd, and Tb) already revealed weak superstructure reflections indicating cell enlargements. Here we report on the palladium–germanium ordering in these equiatomic germanides. CePdGe shows a trippled cell content. It is isotypic with CaCuGe (25) and α-YbAuGe (28). The structures of the two modifications of GdPdGe are both superstructures of the KHg_2 type: the low-temperature α-modification has a tripled cell volume with CaCuGe-type structure, while the high-temperature β-modification has a doubled cell content and is isotypic with YPdSi (24).

While trying to prepare a sample of YbPdGe (8, 17) we obtained the new germanide $Yb_3Pd_4Ge_4$ with $Gd_3Cu_4Ge_4$ ($Li_4Sr_3Sb_4$)-type structure (29, 30) which we refined on the basis of single-crystal data. So far, only $Ho_3Pd_4Ge_4$ (31) and $Tm_3Pd_4Ge_4$ (32) are known in this series. Recent phase analytical investigations indicated also the existence of the other $Ln_3Pd_4Ge_4$ germanides with *Ln* = Y, Gd–Er (33).

EXPERIMENTAL

Starting materials for the preparation of the ternary germanides were ingots of the rare earth elements (Kelpin and Johnson Matthey), palladium powder (Degussa, 200 mesh),

[1] To whom correspondence should be addressed.

0022-4596/00 $35.00

and germanium lumps (Wacker), all with stated purities better than 99.9%. In the first step, the rare earth ingots were cut into smaller pieces under paraffin oil. The latter was washed off with *n*-hexane and the pieces were kept in Schlenk tubes under argon. The paraffin oil and *n*-hexane were dried over sodium wire and the argon was purified over molecular sieves and titanium sponge (900 K). The rare earth pieces were then arc-melted to small buttons (about 500 mg) in a miniaturized arc-melting furnace (34). This premelting procedure greatly reduces shattering of these elements during the exothermic reaction. The palladium powder was pressed to small pellets (6 mm diameter).

The rare earth buttons, the palladium pellets, and the germanium lumps were then mixed in the ideal atomic ratio 1 : 1 : 1 and melted in an arc furnace under an argon pressure of about 600 mbar. The melted ingots were turned over and remelted three times on each side to ensure homogeneity. With the exception of the gadolinium compound, all samples were subsequently enclosed in evacuated silica tubes and annealed at 1070 K for 2 weeks. GdPdGe is dimorphic. The high-temperature modification β-GdPdGe is obtained by quenching, while the low-temperature modification α-GdPdGe forms upon annealing β-GdPdGe for 4 weeks at 1070 K. High-quality single crystals of β-GdPdGe were obtained by annealing an arc-melted button slightly below the melting point for 2 hours in a water-cooled silica tube using a high-frequency generator. The experimental setup is shown in Fig. 1.

Due to the low boiling point of ytterbium (1700 K), $Yb_3Pd_4Ge_4$ could not be prepared by arc-melting. The elements were therefore sealed in a small (1 cm^3) tantalum tube under an argon pressure of 600 mbar. The tube was placed in a water-cooled quartz glass sample chamber in a high-frequency furnace (Kontron Roto-Melt, 1.2 kW). The experimental setup has been described in detail elsewhere (35). In the first step, the tube was heated with the maximum power output of the generator. The exothermic reaction was easily noted by observing the occurence of white heat for about 1 second. The annealing temperature was then lowered to about 1100 K for about 1 minute and then raised again to the maximum. Subsequently the tube was annealed for 3 hours at about 1100 K. The reaction resulted in a light-gray polycrystalline sample of $Yb_3Pd_4Ge_4$ which could easily be separated from the tantalum tube. Using this preparation technique, it was only possible to obtain samples with a $Yb_3Pd_4Ge_4$ content of about 90%. We always observed a small amount of equiatomic YbPdGe as a second phase in our samples.

The silvery ingots of *Ln*PdGe and $Yb_3Pd_4Ge_4$ were well crystallized and extremely brittle. The polycrystalline samples are stable in moist air over a period of several months. No deterioration could be observed. Powders are dark gray. The irregularly shaped single crystals exhibit a metallic luster.

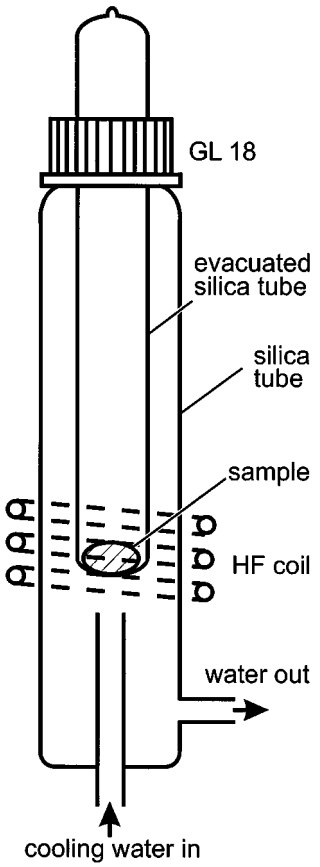

FIG. 1. Experimental setup for the inductive annealing of an ingot in a water-cooled silica tube.

The purity of the samples was checked by Guinier powder patterns using Cu $K\alpha_1$ radiation and α-quartz ($a = 491.30$ pm, $c = 540.46$ pm) as an internal standard. The lattice constants (Table 1) were obtained by least-squares fits of the powder data. The indexing of the diffraction lines was facilitated by intensity calculations (36) using the positional parameters of the refined structures. All subcell reflections of our Guinier powder data are in good agreement with those reported earlier in the literature (Table 1).

Single-crystal intensity data were collected at room temperature by use of a four-circle diffractometer (Enraf-Nonius CAD4) with graphite-monochromatized Mo $K\alpha$ radiation and a scintillation counter with pulse height discrimination. Empirical absorption corrections were applied on the basis of psi-scan data. Further details of the data collections are listed in Table 2.

RESULTS AND DISCUSSION

Lattice Parameters

In all previous investigations, the germanides *Ln*PdGe were characterized only on the basis of X-ray and neutron

TABLE 1
Lattice Constants of the Germanides *Ln*PdGe (*Ln* = La, Ce, Pr, Nd, Sm, Gd, and Tb) and $Yb_3Pd_4Ge_4$[a]

Compound	Structure type	*a* (pm)	*b* (pm)	*c* (pm)	*V* (nm^3)	Ref.
LaPdGe	CaCuGe	2225.5(2)	451.71(7)	771.67(8)	0.7558(1)	This work
	KHg_2	451.8(1)	740.9(9)	774.0(4)	0.2591(3)	(1)
CePdGe	CaCuGe	2190.2(9)	448.4(2)	767.3(3)	0.7535(1)	This work
	KHg_2	448.73(9)	730.5(1)	767.9(2)	0.25172(9)	(1)
	KHg_2	448.75(7)	730.0(3)	767.6(3)	0.2515(1)	(3)
	KHg_2	448.7	730.5	767.9	0.2517	(7)
	KHg_2	446.8(2)	725.5(4)	764.4(4)	0.2478(1)	(14)
	KHg_2	448.0(4)	728.8(5)	767.2(4)	0.2505(1)	(16)
PrPdGe	CaCuGe	2177.4(6)	447.8(2)	766.4(2)	0.7472(1)	This work
	KHg_2	447.2(3)	725.6(2)	765.4(3)	0.2484(2)	(1)
	KHg_2	446.8	725.0	765.7	0.2480	(7)
	KHg_2	460.6(1)	722.0(3)	764.1(2)	0.2541(1)	(14)
NdPdGe	CaCuGe	2160.8(3)	445.6(1)	763.9(1)	0.7356(1)	This work
	KHg_2	445.4(1)	720.5(2)	763.9(3)	0.2451(1)	(1)
	KHg_2	445.8	720.5	764.2	0.2455	(7)
SmPdGe	CaCuGe	2133.8(3)	442.7(1)	760.2(1)	0.7182(1)	This work
	KHg_2	442.63(9)	711.0(1)	760.6(2)	0.23937(9)	(1)
	KHg_2	442.6	711.0	760.6	0.2394	(15)
α-GdPdGe	CaCuGe	2112.3(3)	440.5(1)	757.7(1)	0.7051(1)	This work
β-GdPdGe	YPdSi	440.3(1)	1409.9(2)	757.6(1)	0.4703(1)	This work
GdPdGe	KHg_2	440.6(1)	705.4(2)	757.7(2)	0.2355(1)	(1)
	KHg_2	439.8	704.4	757.0	0.2345	(7)
TbPdGe	YPdSi	438.9(9)	1398.2(3)	756.4(2)	0.4641(1)	This work
	KHg_2	438.1(1)	700.0(2)	757.3(2)	0.2322(1)	(1)
	KHg_2	438.1	700.0	757.3	0.2322	(7)
	KHg_2	437.0(4)	696.1(7)	755.2(7)	0.2297(1)	(14)
$Yb_3Pd_4Ge_4$	$Gd_3Cu_4Ge_4$	410.7(1)	707.0(1)	1372.2(3)	0.3984(1)	This work

[a] Standard deviations in the positions of the last significant digits are given in parentheses throughout the paper. The settings of the three different structures of the equiatomic compounds have the following relations: *abc* (KHg_2) ~ 3*bac̄* (CaCuGe) ~ *a*2*bc* (YPdSi). The data reported in Ref. (14) were collected at low temperatures.

powder diffraction data. These powder patterns were indexed on the basis of small orthorhombic body-centered cells.

Motivated by our recent studies on various KHg_2 superstructures (22–27), we reinvestigated also the powder patterns of the germanides *Ln*PdGe. With the various known superstructure models it was possible to generate theoretical powder diagrams (36). This procedure was helpful in assigning the correct structure type on the basis of X-ray powder

TABLE 2
Crystal Data and Results of the Structure Refinements for CePdGe, α-GdPdGe, β-GdPdGe, and $Yb_3Pd_4Ge_4$

Empirical formula	CePdGe	α-GdPdGe	β-GdPdGe	$Yb_3Pd_4Ge_4$
Pearson symbol	*oP*36	*oP*36	*oP*24	*oI*22
Molar mass	319.11	336.24	336.24	1235.08
Calculated density (g/cm^3)	8.44	9.50	9.50	10.30
Formula units/cell	12	12	8	2
Space group	*Pnma* (No. 62)	*Pnma* (No. 62)	*Pmmn* (No. 59)	*Immm* (No. 71)
Crystal size (μm^3)	10 × 40 × 40	10 × 40 × 40	20 × 20 × 40	20 × 30 × 40
Transm. ratio (max/min)	1.83	2.29	1.73	2.34
Limiting 2θ	60°	60°	60°	80°
Range in *h*,*k*,*l*	± 30, 0–6, ± 10	0–29, ± 6, ± 10	0–6, ± 19, 0–10	0–7, ± 12, ± 24
Total no. of reflections	4094	3895	1546	2482
Independent refl. (R_{int} on *I*)	1228 (0.058)	1150 (0.049)	801 (0.032)	739 (0.071)
Refl. with $I > 2\sigma(I)$	396	372	470	667
Variables	56	56	40	23
Final residual *R*(*F*)	0.019	0.022	0.019	0.027
Weighted *R* (F^2, all data)	0.042	0.053	0.061	0.078
Goodness-of-fit on F^2	0.934	0.941	1.034	1.199
Largest diff. peak/hole (e/Å^3)	1.97/ − 2.01	1.67/ − 2.24	1.53/ − 1.66	3.93/ − 4.32

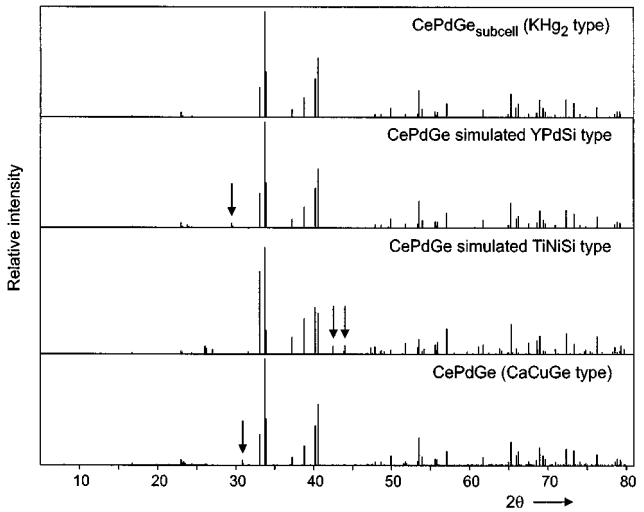

FIG. 2. Calculated powder patterns (Cu $K\alpha_1$ radiation) for the KHg_2-type subcell and the CaCuGe-type superstructure of CePdGe. The other two diagrams are simulations for a possible YPdSi- or TiNiSi-type superstructure for CePdGe. The unequivocal superstructure reflections for each superstructure model are marked by arrows.

data. The Guinier patterns of arc-melted and of annealed CePdGe showed some weak additional reflections which could be attributed to a palladium–germanium ordering as realized in the CaCuGe-type structure. The four strongest superstructure reflections of CePdGe, i.e., 111, 102, 511, and 502 have calculated intensities (in %) of 2.7, 1.2, 3.9, and 1.2 with respect to the strongest subcell reflection. In Fig. 2 we present the calculated powder diagrams for the subcell and the CaCuGe-type superstructure of CePdGe. For comparison also the simulated diagrams for a possible TiNiSi and YPdSi superstructure are shown. It can be seen that these three different KHg_2 superstructures can clearly be distinguished from high quality X-ray powder data.

Structure Refinements

Single crystals of CePdGe, α-GdPdGe, β-GdPdGe, and $Yb_3Pd_4Ge_4$ were isolated from the crushed samples and examined by Buerger precession photographs to establish both symmetry and suitability for the intensity data collections. The photographs of CePdGe, α-GdPdGe, and β-GdPdGe showed pronounced KHg_2-like orthorhombic subcells with Laue symmetry *mmm* and weak superstructure reflections which require a trippling of the subcell *b* axis for CePdGe and α-GdPdGe and a doubling for β-GdPdGe. Similar cell enlargements have recently been observed for the CaCuGe-type silicides α-GdPdSi (26) and YPdSi-type β-GdPdSi (24), respectively. The extinction conditions were compatible with space group *Pnma* for CePdGe and α-GdPdGe, and *Pmmn* for β-GdPdGe. The precession films of $Yb_3Pd_4Ge_4$ showed Laue symmetry *mmm* and the only systematic extinctions were those of a body-centered lattice in agreement with space group *Immm*. All relevant crystallographic data and experimental details are listed in Table 2.

The atomic parameters of CaCuGe (25) and CePtGe (27) were taken as starting parameters for the refinements of the structures of CePdGe, α-GdPdGe, and β-GdPdGe, while those for $Yb_3Pd_4Ge_4$ were obtained from direct methods using the program package Shelx-97 (37). The four structures were then successfully refined using a full-matrix least-squares program of the same package with anisotropic displacement parameters for all atoms. As checks for the correct site assignments and the correct compositions, the occupancy parameters were varied in separate series of least-squares cycles. All positions were found to be fully occupied within five standard deviations (Table 3). In the final cycles the ideal occupancies were assumed again. Final difference Fourier syntheses were flat. Atomic coordinates and interatomic distances are listed in the Tables 3 and 4. The refinements converged to low residuals. Listings of the anisotropic displacement parameters and the observed and calculated structure factors are available. [Details may be obtained from Fachinformationszentrum Karlsruhe, D-76344 Eggenstein-Leopoldshafen, Germany, by quoting the registry numbers CSD-411184 (CePdGe), CSD-411186 (α-GdPdGe), CSD-411185 (β-GdPdGe), and CSD-411182 ($Yb_3Pd_4Ge_4$).]

Crystal Chemistry of the Germanides LnPdGe

The series of equiatomic *Ln*PdGe germanides has previously been reported to crystallize with KHg_2 ($CeCu_2$)-type structure (1–18) where the palladium and germanium atoms statistically occupy the mercury position of the KHg_2-type structure. The present reinvestigations clearly show that this is only the subcell structure for the compounds with *Ln* = La–Nd, Sm, Gd, and Tb. Our Guinier powder patterns and the X-ray single-crystal investigations unambiguously prove that LaPdGe, CePdGe, PrPdGe, NdPdGe, SmPdGe, and α-GdPdGe crystallize with the centrosymmetric CaCuGe-type (25) structure, space group *Pnma*, with a trippled unit cell, which has also been found for α-YbAuGe (28).

The dimorphism of the gadolinium compound is reported here for the first time. The low-temperature α-modification of GdPdGe with CaCuGe-type structure was obtained by annealing at 1070 K. The high-temperature β-modification forms upon melting and quenching. β-GdPdGe crystallizes with the orthorhombic YPdSi-type structure (24), space group *Pmmn*, with a doubled unit cell. According to our Guinier powder data, also TbPdGe adopts the YPdSi type.

We have also reinvestigated the *Ln*PdGe germanides with *Ln* = Dy–Lu as rare earth components. The powder patterns of these germanides also show pronounced KHg_2-type subcells and some weak additional reflections. However, it was not (yet) possible to determine the

TABLE 3
Atomic Parameters for CePdGe, α-GdPdGe, β-GdPdGe, and $Yb_3Pd_4Ge_4$[a]

Atom	Occupancy	Site	*x*	*y*	*z*	U_{eq}
			CePdGe (*Pnma*)			
Ce1	0.998(5)	4*c*	0.00195(7)	1/4	0.7141(3)	74(5)
Ce2	1.006(4)	4*c*	0.1660(1)	1/4	0.7927(2)	73(3)
Ce3	1.008(4)	4*c*	0.3330(1)	1/4	0.7116(2)	76(3)
Pd1	0.992(6)	4*c*	0.0939(1)	1/4	0.4199(3)	90(6)
Pd2	0.981(6)	4*c*	0.2376(1)	1/4	0.4193(3)	76(5)
Pd3	0.996(6)	4*c*	0.4340(1)	1/4	0.4169(3)	112(6)
Ge1	1.008(8)	4*c*	0.0709(2)	1/4	0.0901(4)	85(7)
Ge2	0.980(8)	4*c*	0.2696(2)	1/4	0.0875(4)	83(7)
Ge3	1.04(1)	4*c*	0.3958(2)	1/4	0.0854(4)	52(7)
			α-GdPdGe (*Pnma*)			
Gd1	1.000(6)	4*c*	0.00100(6)	1/4	0.7137(2)	75(5)
Gd2	0.999(4)	4*c*	0.1660(1)	1/4	0.7916(2)	69(3)
Gd3	1.006(5)	4*c*	0.3330(1)	1/4	0.7119(2)	73(3)
Pd1	0.976(8)	4*c*	0.0938(1)	1/4	0.4205(4)	90(6)
Pd2	1.001(7)	4*c*	0.2367(1)	1/4	0.4197(3)	70(5)
Pd3	1.002(8)	4*c*	0.4355(2)	1/4	0.4178(4)	101(6)
Ge1	1.02(1)	4*c*	0.0723(2)	1/4	0.0894(5)	78(8)
Ge2	1.00(1)	4*c*	0.2677(2)	1/4	0.0887(4)	75(7)
Ge3	1.00(1)	4*c*	0.3974(2)	1/4	0.0876(5)	59(7)
			β-GdPdGe (*Pmmn*)			
Gd1	1.000(3)	4*e*	1/4	0.00172(3)	0.78681(6)	71(2)
Gd2	1.013(3)	2*b*	1/4	3/4	0.71041(9)	70(2)
Gd3	1.011(3)	2*a*	1/4	1/4	0.70352(9)	67(2)
Pd1	0.994(3)	4*e*	1/4	0.14167(6)	0.0773(1)	76(2)
Pd2	0.985(3)	4*e*	1/4	0.59600(6)	0.4182(1)	89(2)
Ge1	0.996(5)	4*e*	1/4	0.10515(8)	0.4088(1)	76(3)
Ge2	0.996(5)	4*e*	1/4	0.65386(7)	0.0899(1)	71(3)
			$Yb_3Pd_4Ge_4$ (*Immm*)			
Yb1	0.997(2)	4*j*	1/2	0	0.37408(3)	55(1)
Yb2	1.008(3)	2*a*	0	0	0	88(1)
Pd	0.999(3)	8*l*	0	0.29914(6)	0.32441(4)	66(1)
Ge1	1.014(5)	4*i*	0	0	0.21976(8)	61(2)
Ge2	1.008(5)	4*h*	0	0.1811(1)	1/2	61(2)

[a] The occupancy parameters were obtained in separate series of least-square cycles. In the final cycles the ideal occupancy parameters were used. U_{eq} (pm^2) is defined as one-third of the trace of the orthogonalized U_{ij} tensor.

palladium–germanium ordering for these compounds. The observed additional reflections did not correspond with those of the known superstructures. For example, single-crystal film and diffractometer data of YbPdGe show a doubling of all three subcell axes. Detailed structure analyses of these *Ln*PdGe compounds are now in progress.

The structures of CePdGe, PrPdGe, NdPdGe, GdPdGe, and TbPdGe have recently also been investigated by neutron powder diffraction (7, 14, 18); however, no indications for superstructure reflections were reported. This can most likely be attributed to too small counting times or to deviations from the ideal composition *Ln*PdGe. Small homogeneity ranges with Pd/Ge substition of the type $LnPd_{1-x}Ge_{1+x}$ or $LnPd_{1+x}Ge_{1-x}$ may possibly prevent long-range order and then only the KHg_2-type subcell structure may be observed by X-ray or neutron diffraction.

The refinement of the occupancy parameters during our previous single-crystal investigations of the series of *Ln*PtGe germanides (27) and α-GdPdSi (26) revealed some platinum/germanium (palladium/silicon) disorder also in the superstructures. Such a slight disorder is also indicated by the occupancy parameters listed in Table 3. The standard deviations for the individual occupancy parameters are so large that all occupancy parameters seem to be at the ideal values within five standard deviations. However, when comparing the average occupancy parameters for the four structures (including $Yb_3Pd_4Ge_4$) we note a pronounced tendency: the ratio of the occupancy parameters of the average palladium and the average germanium positions

TABLE 4
Interatomic Distances, Calculated with the Lattice Constants Taken from the X-Ray Powder Data[a]

	CePdGe	
Ce1:1 Pd1 302.4(4)	Ce2:2 Ge3 306.4(3)	Ce3:1 Pd2 306.4(3)
2 Pd3 306.9(2)	2 Ge2 308.2(3)	2 Pd2 315.5(2)
2 Ge1 313.6(3)	1 Ge1 309.0(5)	1 Pd3 316.4(4)
1 Pd3 319.8(4)	1 Ge2 320.3(4)	1 Ge3 318.1(4)
2 Pd1 323.8(2)	2 Pd2 322.9(3)	2 Pd1 318.6(3)
1 Ge1 325.7(5)	1 Pd2 326.6(4)	1 Ge2 320.1(4)
1 Ge3 326.9(4)	1 Pd1 326.8(4)	2 Ge1 321.4(3)
2 Ge3 331.9(3)	2 Pd3 327.7(3)	2 Ge2 331.3(3)
1 Ce2 364.4(3)	1 Ce1 364.4(3)	1 Ce2 370.9(5)
1 Ce3 374.5(3)	1 Ce3 370.9(5)	1 Ce1 374.5(3)
2 Ce1 397.8(4)	2 Ce3 391.9(2)	2 Ce2 391.9(2)
Pd1:1 Ge1 258.0(3)	Pd2:2 Ge2 259.2(2)	Pd3:2 Ge1 260.8(2)
2 Ge3 258.6(2)	1 Ge2 264.1(4)	1 Ge3 267.9(3)
1 Ce1 302.4(4)	1 Ce3 306.4(3)	1 Ge1 299.8(6)
1 Pd2 314.9(3)	1 Pd1 314.9(3)	2 Ce1 306.9(2)
2 Ce3 318.6(3)	2 Ce3 315.5(2)	1 Ce3 316.4(4)
2 Ce1 323.8(2)	2 Ce2 322.9(3)	1 Ce1 319.8(4)
1 Ce2 326.8(4)	1 Ce2 326.6(4)	2 Ce2 327.7(3)
Ge1:1 Pd1 258.0(3)	Ge2:2 Pd2 259.2(2)	Ge3:2 Pd1 258.6(2)
2 Pd3 260.8(2)	1 Pd2 264.1(4)	1 Pd3 267.9(3)
1 Pd3 299.8(6)	1 Ge3 276.5(4)	1 Ge2 276.5(4)
1 Ce2 309.0(5)	2 Ce2 308.2(3)	2 Ce2 306.4(3)
2 Ce1 313.6(3)	1 Ce3 320.1(4)	1 Ce3 318.1(4)
2 Ce3 321.4(3)	1 Ce2 320.3(4)	1 Ce1 326.9(4)
1 Ce1 325.7(5)	2 Ce3 331.3(3)	2 Ce1 331.9(3)
	α-GdPdGe	
Gd1:1 Pd1 296.3(3)	Gd2:1 Ge1 300.2(5)	Gd3:1 Pd2 300.7(3)
2 Pd3 300.7(2)	2 Ge3 300.6(3)	2 Pd2 308.2(2)
2 Ge1 307.8(3)	2 Ge2 303.0(3)	1 Pd3 310.7(4)
1 Pd3 311.6(4)	1 Ge2 311.1(4)	2 Ge1 311.7(3)
2 Pd1 314.6(2)	2 Pd2 316.4(3)	2 Pd1 312.0(3)
1 Ge3 316.3(4)	1 Pd2 318.9(3)	1 Ge3 315.5(4)
1 Ge1 322.0(4)	1 Pd1 319.9(3)	1 Ge2 317.1(4)
2 Ge3 322.0(3)	2 Pd3 322.0(3)	2 Ge2 320.1(3)
1 Gd2 353.5(2)	1 Gd1 353.5(2)	1 Gd2 357.9(5)
1 Gd3 359.3(3)	1 Gd3 357.9(5)	1 Gd1 359.3(3)
2 Gd1 391.6(3)	2 Gd3 387.2(2)	2 Gd2 387.2(2)
Pd1:2 Ge3 254.8(3)	Pd2:2 Ge2 255.0(2)	Pd3:2 Ge1 256.3(3)
1 Ge1 255.0(3)	1 Ge2 259.2(5)	1 Ge3 262.8(4)
1 Gd1 296.3(3)	1 Gd3 300.7(3)	1 Ge1 288.9(6)
1 Pd2 301.8(3)	1 Pd1 301.8(3)	2 Gd1 300.7(2)
2 Gd3 312.0(2)	2 Gd3 308.2(2)	1 Gd3 310.7(4)
2 Gd1 314.6(2)	2 Gd2 316.4(3)	1 Gd1 311.6(4)
1 Gd2 319.9(3)	1 Gd2 318.9(3)	2 Gd2 322.0(3)
Ge1:1 Pd1 255.0(3)	Ge2:2 Pd2 255.0(2)	Ge3:2 Pd1 254.8(3)
2 Pd3 256.3(3)	1 Pd2 259.2(5)	1 Pd3 262.8(4)
1 Pd3 288.9(6)	1 Ge3 274.1(4)	1 Ge2 274.1(4)
1 Gd2 300.2(5)	2 Gd2 303.0(3)	2 Gd2 300.6(3)
2 Gd1 307.8(3)	1 Gd2 311.1(4)	1 Gd3 315.5(4)
2 Gd3 311.7(3)	1 Gd3 317.1(4)	1 Gd1 316.3(4)
1 Gd1 322.0(4)	2 Gd3 320.1(3)	2 Gd1 322.0(3)
	β-GdPdGe	
Gd1:1 Pd1 295.6(1)	Gd2:2 Pd2 310.1(1)	Gd3:4 Ge2 302.2(1)
2 Pd2 300.4(1)	4 Pd1 312.5(1)	2 Ge1 302.6(1)
2 Ge1 305.2(1)	4 Ge1 313.6(1)	2 Pd1 321.7(1)
1 Pd2 311.4(1)	2 Ge2 317.9(1)	4 Pd2 322.7(1)
2 Pd1 316.1(1)	2 Gd1 359.6(1)	2 Gd1 355.7(1)
1 Ge2 317.6(1)	2 Gd3 383.2(1)	2 Gd2 383.2(1)
2 Ge2 321.2(1)		
1 Ge1 321.4(1)	Pd1:2 Ge2 254.6(1)	Pd2:2 Ge1 256.5(1)
1 Gd3 355.7(1)	1 Ge1 256.4(1)	1 Ge2 261.7(1)
1 Gd2 359.6(1)	1 Gd1 295.6(1)	1 Ge1 283.7(1)
2 Gd1 391.0(1)	1 Pd1 305.5(2)	2 Gd1 300.4(1)
	2 Gd2 312.5(1)	1 Gd2 310.1(1)
	2 Gd1 316.1(1)	1 Gd1 311.4(1)
	1 Gd3 321.7(1)	2 Gd3 322.7(1)
	Ge1:1 Pd1 256.4(1)	Ge2:2 Pd1 254.6(1)
	2 Pd2 256.5(1)	1 Pd2 261.7(1)
	1 Pd2 283.7(1)	1 Ge2 271.1(2)
	1 Gd3 302.6(1)	2 Gd3 302.2(1)
	2 Gd1 305.2(1)	1 Gd1 317.6(1)
	2 Gd2 313.6(1)	1 Gd2 317.9(1)
	1 Gd1 321.4(1)	2 Gd1 321.3(1)
	$Yb_3Pd_4Ge_4$	
Yb1:2 Ge1 295.0(1)	Yb2:2 Ge1 301.6(1)	Ge1:2 Pd 255.6(1)
4 Ge2 297.4(1)	4 Ge2 305.0(1)	4 Pd 256.9(1)
4 Pd 302.6(1)	8 Pd 347.0(1)	2 Yb1 295.0(1)
2 Pd 307.2(1)	4 Yb1 393.5(1)	1 Yb2 301.6(1)
1 Yb1 345.6(1)	2 Yb2 410.7(1)	2 Yb1 376.2(1)
2 Ge1 376.2(1)		
2 Yb2 393.5(1)	Pd:1 Ge2 255.0(1)	Ge2:2 Pd 255.0(1)
2 Yb1 410.7(1)	1 Ge1 255.6(1)	1 Ge2 256.1(1)
	2 Ge1 256.9(1)	4 Yb1 297.4(1)
	1 Pd 284.0(1)	2 Yb2 305.0(1)
	2 Pd 297.8(1)	
	2 Yb1 302.6(1)	
	1 Yb1 307.2(1)	
	2 Yb2 347.0(1)	

[a] All distances shorter than 440 pm (coordinations of the *Ln* atoms), 370 pm (Pd), and 380 pm (Ge) are listed.

Pd/Ge is always smaller than one, i.e., 0.990/1.009 for CePdGe, 0.993/1.007 for α-GdPdGe, 0.990/0.996 for β-GdPdGe, and 0.999/1.011 for $Yb_3Pd_4Ge_4$. Various rationalizations for this tendency have been discussed earlier (27). Most likely this tendency can be rationalized by assuming a small percentage of palladium positions to be occupied by germanium atoms and *vice versa*, a small percentage of palladium atoms on germanium positions. The corresponding deviations from the ideal occupancy values were found to be larger in the platinum germanides *Ln*PtGe (27) and this correlates with the fact that the difference in the scattering power is greater between platinum and germanium (atomic numbers 78 and 32) than between palladium and germanium (46 and 32).

The structural relationships of the various KHg_2 superstructures have been discussed in detail in several earlier papers (22–27). Here we only briefly consider the crystal chemistry of α-GdPdGe and β-GdPdGe. The near-neighbor coordination of the gadolinium atoms in both modifications

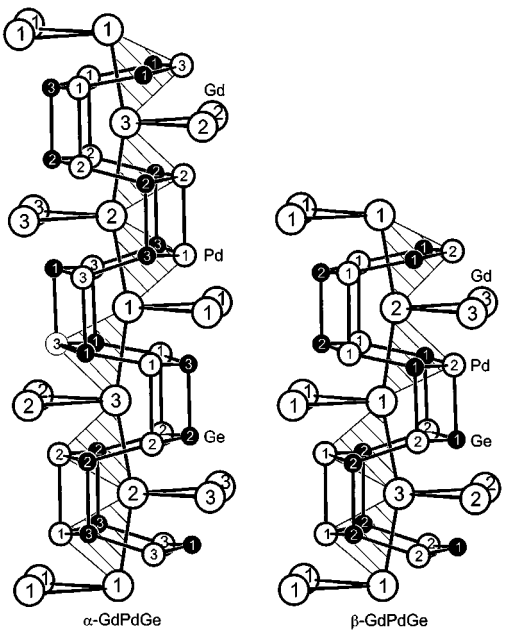

FIG. 3. Near-neighbor environments of the gadolinium atoms in α- and β-GdPdGe. Numbers correspond to the atom designations in Table 3. The counter-tilted hexagonal networks of the palladium and germanium atoms are emphasized. The shaded triangles correspond to the trigonal prisms accentuated in Fig. 4. The drawings show one translation length *a* of α-GdPdGe and one translation length *b* of β-GdPdGe.

is presented in Fig. 3. As emphasized recently (25, 39), the orthorhombically distorted KHg_2 superstructures derive from the aristotype AlB_2. Consequently, each gadolinium atom in α- and β-GdPdGe has a coordination of two slightly puckered and tilted hexagons (Fig. 3). Within the Pd_3Ge_3 hexagons, the Pd–Ge distances range from 255 to 263 pm, only slightly larger than the sum of Pauling's single bond radii (40) of 251 pm for palladium and germanium, indicating strong Pd–Ge interactions. In the third dimension the Pd_3Ge_3 hexagons are linked via longer Pd–Ge (284–289 pm), Pd–Pd (302–306 pm), and Ge–Ge (271–274 pm) bonds. In view of the Pd–Pd and Ge–Ge distances of 275 pm in *fcc* palladium and 245 pm in germanium (41), these interlayer interactions are very weak.

The gadolinium atoms have some palladium and germanium neighbors at the relatively short Gd–Pd and Gd–Ge distances of 296 and 300 pm, respectively. Regarding the sums of Pauling's single bond radii of 289 pm (Gd + Pd) and 283 pm (Gd + Ge), these contacts may also be considered as bonding interactions. In addition, each gadolinium atom has four nearest gadolinium neighbors at Gd–Gd distances ranging from 354 to 392 pm. The two shorter contacts of each gadolinium atom correspond to the Gd–Gd *zigzag* chains presented in Fig. 3 and the shaded triangles correspond to the basal planes of the trigonal prisms shown in Fig. 4.

Projections of the α- and β-GdPdGe structures are presented in Fig. 4. From a geometrical point of view, the gadolinium and palladium atoms build chains of slightly distorted trigonal prisms which are centered by the germanium atoms. Adjacent chains are shifted by half a translation period of the projection direction. For each KHg_2-type superstructure, the chains of trigonal prisms have distinct ordering sequences. The orientations of the trigonal prisms are labeled + if the palladium edges point in the $+z$ direction and the label − is assigned if they point in the opposite direction. Thus, α-GdPdGe has the ordering sequence $+++---$ with six prisms in the corresponding translation period, while the sequence of β-GdPdGe is $++--$ with four prisms per translation period. Both the palladium and the germanium atoms occupy the mercury positions of the KHg_2-type subcell. Hence, the palladium atoms are situated in trigonal prisms formed by the gadolinium and germanium atoms with the analogous sequence as the germanium atoms in the trigonal prisms formed by the gadolinium and palladium atoms. From a topological point of view these two description are equivalent (26). The ordering scheme, designating the orientation of the trigonal

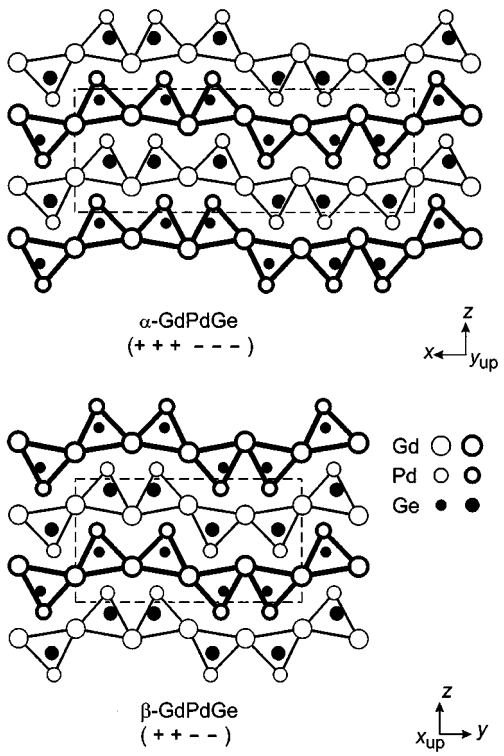

FIG. 4. Projection of the crystal structures of α- and β-GdPdGe along the short axes. All atoms lie on mirror planes which are separated by half a translation period of the projection directions, indicated by thin and thick lines, respectively. The germanium-centered trigonal prisms are outlined. The orientations of the prisms are labeled + if they point in the $+z$ direction and − if they point in the opposite direction.

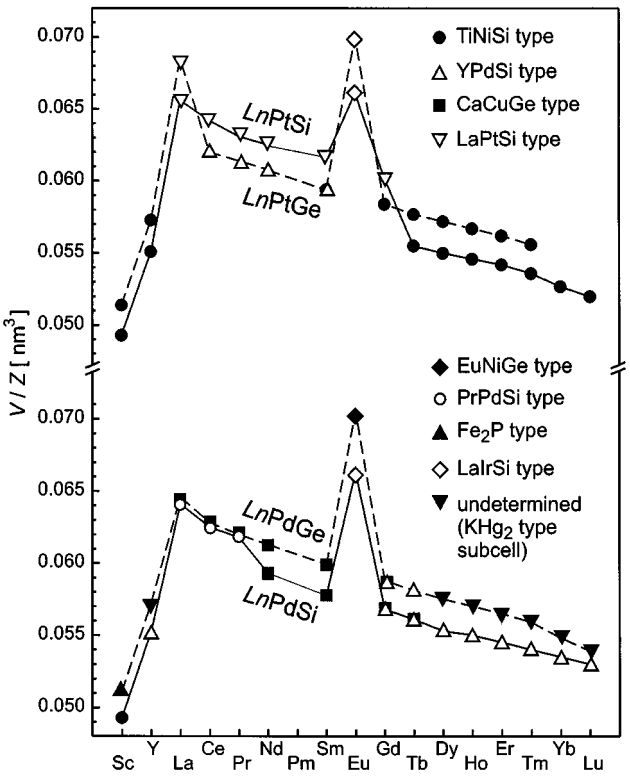

FIG. 5. Cell volumes per formula unit of the four series of silicides and germanides $LnTM$ (T = Pd, Pt; M = Si, Ge).

prisms with + and − signs was initially developed in Ref. (23) in order to distinguish different superstructures of the KHg_2 family.

In Fig. 5 we represent all equiatomic compounds of the four series $LnTM$ (T = Pd, Pt; M = Si, Ge) by their cell volumes per formula unit. The LnPdGe germanides with Ln = La–Nd, Sm, and Gd adopt the CaCuGe type, while β-GdPdGe and TbPdGe crystallize with YPdSi-type structure. Also the corresponding series of platinum germanides LnPtGe (27) and palladium silicides LnPdSi (26) show such changes in the structure types. Very similar to α- and β-GdPdGe also α-GdPdSi (CaCuGe type) and β-GdPdSi (YPdSi type) as well as α-SmPtGe (YPdSi type) and β-SmPtGe (TiNiSi type) show dimorphism. These are the compounds where one series of isotypic structures meets the other.

The New Germanide $Yb_3Pd_4Ge_4$

The phase relationships at 870 K in the ternary system ytterbium–palladium–germanium have recently been investigated by Seropegin *et al.* (9). On the basis of phase analytical studies, these authors reported 10 ternary germanides in this system. Besides equiatomic YbPdGe (8, 9, 17) and $YbPd_2Ge_2$ with $ThCr_2Si_2$-type structure, they characterized Yb_2PdGe_6 with Ce_2CuGe_6-type, $YbPdGe_2$ with $YIrGe_2$-type, and Yb_2PdGe_3 with disordered AlB_2-type structures, and five other phases with as yet unknown structures. The approximate compositions of these phases, however, gave no indication for the existence of $Yb_3Pd_4Ge_4$ reported herein. This might be ascribed to the relatively high annealing temperature of 1100 K used by us for the preparation of $Yb_3Pd_4Ge_4$.

$Yb_3Pd_4Ge_4$ crystallizes with $Gd_3Cu_4Ge_4$-type structure. A projection of this structure along the x axis is shown in Fig. 6. Both ytterbium sites of $Yb_3Pd_4Ge_4$ have high coordination numbers (CN) as is usual for such intermetallic compounds: CN 19 for Yb1 with 8 Ge + 6 Pd + 5 Yb and CN 20 for Yb2 with 6 Ge + 8 Pd + 6 Yb. The six nearest germanium neighbors of both ytterbium sites have Yb–Ge distances ranging from 295 to 305 pm. These contacts are most likely bonding. Although the coordination numbers of both ytterbium sites are similar, there occur significant differences for the interatomic distances and thus the size of the coordination polyhedra. As outlined in the right-hand part of Fig. 6, the Yb1 atoms (Wyckoff site 4*i*) are located in a smaller cage when compared with the Yb2 atoms (Wyckoff site 2*a*). If we neglect the rather large Yb1–Ge1 distances of 376 pm and consider for both the Yb1 and Yb2 positions only the six nearest Yb–Ge distances we obtain average Yb–Ge, Yb–Pd, and Yb–Yb distances of 297 pm, 304 pm, and 391 pm for Yb1 which are all smaller than the corresponding distances for Yb2 with 304 pm, 347 pm, and 399 pm, respectively. The most significant difference between both ytterbium sites is the average Yb–Pd distance. A quite similar situation occurs in the structure of mixed-valent $Yb_2Pt_3Sn_5$ (35) as well as in α- and β-YbPdSn (42). Considering the possibility of mixed-valent behavior of the ytterbium atoms, one might speculate (since no magnetic

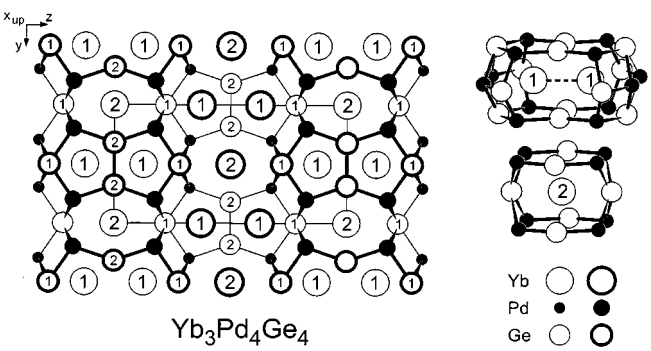

FIG. 6. Crystal structure of $Yb_3Pd_4Ge_4$ and coordination polyhedra of the ytterbium atoms. Atom designations are given in arabic numbers. All atoms lie on mirror planes at $x = 0$ and $x = 1/2$, indicated by thin and thick lines, respectively. The three-dimensional $[Pd_4Ge_4]$ polyanion is emphasized. The cagelike environments of the two crystallographically different ytterbium positions are outlined in the right-hand part of the figure.

data are available) whether or not the Yb1 site is occupied with smaller Yb^{III} and the Yb2 site with larger Yb^{II} atoms as is the case for $Yb_2Pt_3Sn_5$ (35). In this context, the short Yb1–Yb1 distance of 346 pm is especially remarkable. The latter is significantly shorter than the Yb–Yb distance of 388 pm in *fcc* ytterbium (41) and also shorter than those in YbPdSn (42) and $Yb_2Pt_3Sn_5$ (35). A bonding Yb1–Yb1 interaction can only be assumed if the Yb1 atoms have retained some electrons. This supports a lower (at least partial) valence state than III for the Yb1 atoms.

The palladium atoms, all on one crystallographic site, have *CN* 12 with four germanium, three palladium, and five ytterbium neighbors. Different coordination numbers occur for the germanium atoms: *CN* 11 with 6 Pd + 5 Yb for Ge1 and *CN* 9 with 2 Pd + 1 Ge + 6 Yb for Ge2. The latter coordination polyhedron is a nearly regular tricapped trigonal prism as is frequently observed for such intermetallic compounds. The shortest interatomic distances in $Yb_3Pd_4Ge_4$ occur between the palladium and germanium atoms. The average Pd–Ge distance of 256 pm is only slightly larger than the sum of Pauling's single bond radii (40) of 251 pm for palladium and germanium, indicating strong Pd–Ge interactions. These Pd–Ge distances are essentially identical with those in the equiatomic germanides discussed above. In addition, we observe weak Pd–Pd (284 pm) and Ge–Ge (256 pm) contacts in the $Yb_3Pd_4Ge_4$ structure. Again, these distances are only slightly longer than those in *fcc* palladium (275 pm) and elemental germanium (245 pm) (41). Chemical bonding in $Yb_3Pd_4Ge_4$ is thus governed by strong, essentially covalent, Pd–Ge and weak Pd–Pd and Ge–Ge bonding interactions.

ACKNOWLEDGMENTS

We thank Dipl.-Ing. U. Ch. Rodewald for the single-crystal data collections. We are also greatful to Dr. W. Gerhartz (Degussa) and Dr. G. Höfer (Heraeus Quarzschmelze) for generous gifts of palladium and silica tubes, respectively. This work was supported by the Bennigsen-Foerder-Programm of the Ministerium für Wissenschaft und Forschung des Landes Nordrhein-Westfalen, the DAAD, the Heinrich Hertz-Stiftung, the Deutsche Forschungsgemeinschaft, the Fonds der Chemischen Industrie, and the International Centre for Diffraction Data.

REFERENCES

1. E. Hovestreydt, N. Engel, K. Klepp, B. Chabot, and E. Parthé, *J. Less-Common Met.* **85,** 247 (1982).
2. E. Hovestreydt, *J. Less-Common Met.* **143,** 25 (1988).
3. P. Rogl, B. Chevalier, M. J. Besnus, and J. Etourneau, *J. Magn. Magn. Mater.* **80,** 305 (1989).
4. B. Chevalier, P. Rogl, J. Etourneau, and M. J. Besnus, *J. Magn. Magn. Mater.* **83,** 303 (1990).
5. J. Sakurai, Y. Yamaguchi, S. Nishigori, T. Suzuki, and T. Fujita, *J. Magn. Magn. Mater.* **90 & 91,** 422 (1990).
6. M. J. Besnus, A. Braghta, N. Hamdaoui, and A. Meyer, *J. Magn. Magn. Mater.* **104–107,** 1385 (1992).
7. P. A. Kotsanidis, J. K. Yakinthos, E. Roudaut, and H. Gamari-Seale, *J. Magn. Magn. Mater.* **131,** 139 (1994).
8. V. N. Nikiforov, M. V. Kovachikova, A. A. Velikhovskii, Yu. V. Kochetkov, I. Mirkovich, O. M. Borisenko, and Yu. D. Seropegin, *Fiz. Tverd. Tela.* **36,** 471 (1994).
9. Yu. D. Seropegin, O. L. Borisenko, O. I. Bodak, V. N. Nikiforov, M. V. Kovachikova, and Yu. V. Kochetkov, *J. Alloys Compd.* **216,** 259 (1994).
10. R. Pöttgen, *Z. Naturforsch. b* **50,** 1181 (1995).
11. A. V. Morozkin and Yu. D. Seropegin, *J. Alloys Compd.* **237,** 124 (1996).
12. Zh. M. Barakatova, Yu. D. Seropegin, O. I. Bodak, and B. D. Belan, *Inorg. Mater.* **32,** 581 (1996).
13. O. Sologub, K. Hiebl, P. Rogl, and H. Noël, *J. Alloys Compd.* **245,** L13 (1996).
14. A. Szytuła, M. Kolenda, E. Ressouche, and A. Zygmunt, *J. Alloys Compd.* **259,** 36 (1997).
15. Zh. M. Kurenbaeva, Yu. D. Seropegin, O. I. Bodak, and V. N. Nikiforov, *J. Alloys Compd.* **269,** 151 (1998).
16. Yu. D. Seropegin, A. V. Gribanov, and O. I. Bodak, *J. Alloys Compd.* **269,** 157 (1998).
17. Y. Itoh and H. Kadomatsu, *J. Alloys Compd.* **280,** 39 (1998).
18. B. Penc, M. Hofmann, A. Szytuła, and A. Zygmunt, *J. Alloys Compd.* **282,** 52 (1999).
19. E. J. Duwell and N. C. Baenziger, *Acta Crystallogr.* **8,** 705 (1955).
20. A. C. Larson and D. T. Cromer, *Acta Crystallogr.* **14,** 73 (1961).
21. J.-Y. Saillard, J.-F. Halet, R. Müllmann, C. Rosenhahn, B. D. Mosel, R. Pöttgen, and G. Kotzyba, manuscript in preparation.
22. R. Pöttgen, *J. Mater. Chem.* **5,** 505 (1995).
23. R. Pöttgen, R.-D. Hoffmann, R. Müllmann, B. D. Mosel, and G. Kotzyba, *Chem. Eur. J.* **3,** 1852 (1997).
24. Yu. M. Prots', R. Pöttgen, and W. Jeitschko, *Z. Anorg. Allg. Chem.* **624,** 425 (1998).
25. D. Kußmann, R.-D. Hoffmann, and R. Pöttgen, *Z. Anorg. Allg. Chem.* **624,** 1727 (1998).
26. Yu. M. Prots' and W. Jeitschko, *J. Solid State Chem.* **142,** 130 (1999).
27. Yu. M. Prots', R. Pöttgen, D. Niepmann, M. W. Wolff, and W. Jeitschko, *J. Solid State Chem.* **142,** 400 (1999).
28. F. Merlo, M. Pani, F. Canepa, and M. L. Fornasini, *J. Alloys Compd.* **264,** 82 (1998).
29. W. Rieger, *Monatsh. Chem.* **101,** 449 (1970).
30. O. Liebrich, H. Schäfer, and A. Weiss, *Z. Naturforsch. b* **25,** 650 (1970).
31. R. E. Gladyshevskii, O. L. Sologub, and E. Parthé, *J. Alloys Compd.* **176,** 329 (1991).
32. Yu. M. Prots', O. I. Bodak, V. K. Pecharsky, P. S. Salamakha, and Yu. D. Seropegin, *Z. Kristallogr.* **205,** 331 (1993).
33. P. Salamakha, O. Sologub, J. K. Yakinthos, and Ch. D. Routsi, *J. Alloys Compd.* **267,** 192 (1998).
34. R. Pöttgen, Th. Gulden, and A. Simon, *GIT-Laborfachzeitschrift* **43,** 133 (1999).
35. R. Pöttgen, A. Lang, R.-D. Hoffmann, B. Künnen, G. Kotzyba, R. Müllmann, B. D. Mosel, and C. Rosenhahn, *Z. Kristallogr.* **214,** 143 (1999).
36. K. Yvon, W. Jeitschko, and E. Parthé, *J. Appl. Crystallogr.* **10,** 73 (1977).
37. G. M. Sheldrick, SHELX-97, A Program System for the Determination and Refinement of Crystal Structures, University of Göttingen, Germany, 1997.
38. W. Dörrscheidt, N. Niess, and H. Schäfer, *Z. Naturforsch. b* **32,** 985 (1977).
39. R. Pöttgen and R.-D. Hoffmann, *Z. Kristallogr.*, submitted.
40. L. Pauling, "The Nature of the Chemical Bond and the Structures of Molecules and Crystals." Cornell Univ. Press, Ithaca, NY, 1960.
41. J. Donohue, "The Structures of the Elements." Wiley, New York, 1974.
42. D. Kußmann, R. Pöttgen, B. Künnen, G. Kotzyba, R. Müllmann, and B. D. Mosel, *Z. Kristallogr.* **213,** 356 (1998).